Scientific Research Publishing

Journal of Applied Mathematics and Physics, 2026, 14(7), 2533-2549
https://www.scirp.org/journal/jamp
ISSN Online: 2327-4379
ISSN Print: 2327-4352

Population Dynamics System with Time Delay and Taxis

Yangxu Wei

College of Mathematics and Statistics, Northwest Normal University, Lanzhou, China
Email: weiyangxu2026@163.com

How to cite this paper: Wei, Y.X. (2026) Population Dynamics System with Time Delay and Taxis. *Journal of Applied Mathematics and Physics*, **14**, 2533-2549.
https://doi.org/10.4236/jamp.2026.147126

Received: June 4, 2026
Accepted: July 14, 2026
Published: July 17, 2026

Abstract

This paper investigates a class of population dynamics models incorporating prey-taxis, a complex density-dependent functional response, and a time delay in predation conversion. The main purpose of this paper is to explore the effect of time delay on the spatiotemporal dynamic evolution of the system. By fixing the taxis coefficient and conducting a detailed analysis of the characteristic equation of the system at the positive equilibrium point, we treat the time delay τ as the bifurcation parameter, provide sufficient conditions for the local asymptotic stability of the positive equilibrium point in the ODE model, and rigorously prove that delay-induced Hopf bifurcations occur when τ crosses a series of critical thresholds. Finally, numerical simulations verify the correctness of the theoretical analysis. The results indicate that even in a system with spatial diffusion and taxis, a relatively large time delay will destroy the steady-state coexistence of populations, thereby triggering sustained periodic oscillations in predator and prey densities.

Keywords

Predator-Prey Model, Chemotaxis, Time Delay, Hopf Bifurcation

1. Introduction

In ecology and biomathematics, dynamical systems describing the interactions between populations have long attracted significant attention from scholars. In early theoretical studies, researchers typically considered the irregular, random movement of species in space, thereby introducing the mechanism of spatial random diffusion [1].

However, in real natural environments, population movement often exhibits strong directional characteristics. For example, in search of food, predators will spontaneously move toward areas with high prey density; conversely, to avoid

predation risks, prey will actively flee toward areas with low predator density. This phenomenon is known as taxis. Compared to purely random diffusion, this taxis mechanism is more in line with realistic ecological scenarios [2]. Chemotaxis refers to the directional movement of cells or organisms in response to chemical stimuli, serving as an effective theoretical and practical tool for describing the spatiotemporal heterogeneity of ecosystems [3] [4]. Classic prey-taxis models typically assume that predators are unconditionally attracted to prey. Furthermore, to better simulate spatial constraints in real ecological environments and prevent overcrowding caused by population aggregation, some improved models have also introduced a group defense mechanism, such that the taxis response automatically stops when the prey density reaches saturation [5] [6].

On the other hand, time delays are also ubiquitous in real-world biological processes. The growth, sexual maturation, and natural death of individual organisms, as well as the transfer process wherein predators digest prey and convert it into energy for their own reproduction, all require a certain amount of physical time [7]. Recent theoretical studies [8] [9] further emphasize that the time delay caused by digestion and gestation is not merely a supplement to mathematical modeling, but an indispensable core biological feature of real predator-prey systems. Mathematically, the presence of a time delay effect implies that the evolutionary dynamics of the system depend not only on the current state but also on historical information from a past period. Existing research has shown that reaction-diffusion systems incorporating time delays can often trigger more diverse dynamic behaviors compared to those without time delays; for example, time delay is a critical factor in inducing temporal periodic oscillations and spatial patterns [10]-[12].

Although a large body of literature has explored spatial Turing patterns induced by taxis [13]-[15] and the unilateral driving effect of time delays in inducing spatially homogeneous periodic patterns under specific conditions [16], research on the spatiotemporal dynamics under their combined effect remains relatively insufficient. In particular, after introducing taxis, the analysis of the system's characteristic operator becomes exceptionally complex. To clearly investigate the oscillatory evolutionary laws of the system, this paper focuses its core research on the Hopf bifurcation phenomenon induced by time delay. Under a rigorous mathematical framework, this paper reconstructs the analytical procedure using time delay as the primary bifurcation parameter, calculates in detail the transversality condition for the characteristic roots crossing the imaginary axis, and successfully derives the critical parameter expression for the occurrence of the Hopf bifurcation in the system.

Based on the above research motivations, we introduce the population dynamics model of cooperative hunting from literature [17]:

$$\begin{cases} \dfrac{\mathrm{d}n}{\mathrm{d}t} = n\left[\sigma\left(1-\dfrac{n}{\kappa}\right) - \dfrac{(1+\alpha p)p}{1+h_1(1+\alpha p)n+h_2(1+\alpha p)n^2}\right], \\ \dfrac{\mathrm{d}p}{\mathrm{d}t} = p\left[\dfrac{(1+\alpha p)n}{1+h_1(1+\alpha p)n+h_2(1+\alpha p)n^2} - 1\right]. \end{cases} \tag{1}$$

Based on this model, we incorporate spatial diffusion, a taxis term, and a time delay term within a one-dimensional space

$$\begin{cases} \dfrac{\partial n}{\partial t} = d_1 \Delta n + n\left[\sigma\left(1-\dfrac{n}{k}\right) - \dfrac{(1+\alpha p)p}{1+h_1(1+\alpha p)n + h_2(1+\alpha p)n^2}\right], & x \in (0,L), t>0, \\ \dfrac{\partial p}{\partial t} = d_2 \Delta p - \chi \nabla \cdot (\phi \nabla n) \\ \quad + p\left[\dfrac{(1+\alpha p)n(x,t-\tau)}{1+h_1(1+\alpha p)n(x,t-\tau) + h_2(1+\alpha p)n(x,t-\tau)^2} - 1\right], & x \in (0,L), t>0, \\ \dfrac{\partial n}{\partial \nu} = \dfrac{\partial p}{\partial \nu} = 0, & x \in \partial\Omega, t>0, \\ n(x,\theta) = n_0(x,\theta) \geq 0, \ p(x,\theta) = p_0(x,\theta) \geq 0, & x \in [0,L], \theta \in [-\tau, 0]. \end{cases} \tag{2}$$

where $n_0(x,\theta)$ and $p_0(x,\theta)$ represent the continuous non-negative initial functions of the prey and predator, respectively, over the historical time interval $[-\tau, 0]$.

Here, $d_1\Delta n$ and $d_2\Delta p$ represent the natural diffusion behaviors of the prey and predator in space, with d_1 and d_2 being the diffusion coefficients of the prey and predator, respectively. $\sigma n\left(1-\dfrac{n}{k}\right)$ is the Logistic growth term representing the population growth of the prey itself in the absence of predators. σ is the intrinsic growth rate, and k is the carrying capacity.

$-\dfrac{(1+\alpha p)np}{1+h_1(1+\alpha p)n + h_2(1+\alpha p)n^2}$ is the functional response function, where $(1+\alpha p)$ represents cooperative hunting; the predator's attack rate depends not only on the number of prey but also increases with the predator's own density p, and α is the cooperation coefficient; h_1 represents the handling time; n^2 in the denominator represents group defense, meaning when the prey density n is extremely large, the n^2 term in the denominator will dominate, causing the overall predation rate to decrease instead, and h_2 represents the group defense coefficient. $p\dfrac{(1+\alpha p)n(x,t-\tau)}{1+h_1(1+\alpha p)n(x,t-\tau) + h_2(1+\alpha p)n(x,t-\tau)^2}$ represents the population growth obtained by the predator through consuming prey, with the core feature being the introduction of $t-\tau$, which biologically represents a gestation delay or predation conversion time delay. After eating the prey, predators must undergo a physiological period τ of digestion, absorption, and gestation before converting it into new predator individuals. $-p$ represents the mortality rate of the predators.

Based on the group defense term in literature [18], let $\phi = n(n-M)p$. When the prey density is low ($n < M$), $\phi > 0$. Predators will be attracted by the prey and actively aggregate toward areas with high prey density; when the prey density is extremely high ($n > M$), $\phi < 0$. Predators recognize that attacking an overly massive group of prey is dangerous, and therefore actively move away. Here, M is the critical threshold at which the group defense takes effect. Note: Group de-

fense has already been mentioned above, but it is entirely different here. The group defense in the reaction term primarily induces local multi-stability or limit cycle oscillations on a temporal level, whereas the group defense in the taxis term is a defense on the level of spatial movement, which is highly prone to inducing strong spatial Turing instability. These two types of defense are complementary to each other, rather than mutually substitutable. In a normal ecological environment, χ, representing the taxis rate, must be greater than zero. To describe the chemotactic behavior of predators aggregating toward the prey, we define the chemotactic flux of the predator as $J_{chemo} = \chi\phi(n,p)\nabla n$. Here, χ is the chemotactic coefficient and ∇n represents the prey concentration gradient, indicating that the predator's direction of movement is guided by the spatial distribution of the prey. According to the divergence theorem, the rate of change in predator density induced by this flux is $-\nabla \cdot J_{chemo} = -\chi\nabla \cdot \left(\phi(n,p)\nabla n\right)$.

To facilitate the subsequent dynamic analysis, we replace the functional response functions with $f(n,p)$ and $g\left(n(x,t-\tau),p\right)$, yielding:

$$\begin{cases} \dfrac{\partial n}{\partial t} = d_1\Delta n + f\left(n(x,t),p(x,t)\right), & x\in(0,L),t>0, \\ \dfrac{\partial p}{\partial t} = d_2\Delta p - \chi\nabla\cdot(\phi\nabla p) + g\left(n(x,t-\tau),p(x,t)\right), & x\in(0,L),t>0, \\ \dfrac{\partial n}{\partial \nu} = \dfrac{\partial p}{\partial \nu} = 0, & x\in\partial\Omega,t>0, \\ n(x,\theta) = n_0(x,\theta)\geq 0,\ \ p(x,\theta) = p_0(x,\theta)\geq 0, & x\in[0,L],\theta\in[-\tau,0]. \end{cases} \tag{3}$$

Based on the above background, this paper establishes and investigates a class of reaction-diffusion population dynamics models incorporating both time delay and taxis. The main structure of this paper is organized as follows: First, in Section 2, we determine the equilibrium points of model (1) along with their stability conditions, and conduct a rigorous stability analysis of model (3). In Section 3, by calculating the characteristic equation at the positive equilibrium point, we treat the time delay as the key bifurcation parameter and derive the specific mathematical conditions for the occurrence of Hopf bifurcations. Next, in Section 4, we will carry out detailed numerical simulations to verify the aforementioned theoretical predictions.

To highlight the novelty of this work, we contrast our model with closely related literatures. Specifically, literature [16] considered delay-induced patterns but omitted taxis and cooperative hunting. Literature [18] analyzed a 1D prey-taxis system without predation delay or hunting cooperation. Although literature [19] included both delay and cooperative hunting, it lacked spatial diffusion and chemotactic fluxes. Unlike these models focusing on partial mechanisms, this paper simultaneously integrates cooperative hunting, group-defense-regulated chemotactic flux, and predation delay within a unified 1D reaction-diffusion-taxis framework. This comprehensive integration enables us to rigorously analyze the characteristic equations and verify transversality conditions, thereby distinguishing spatially homogeneous and inhomogeneous Hopf bifurcations and clarifying the transition from tem-

poral oscillations to spatial wave-like patterns.

2. Prerequisite Knowledge and Stability Analysis

Before introducing spatial diffusion, taxis, and time delay, we first need to ensure that the corresponding spatially homogeneous ordinary differential equation has a positive equilibrium point $\overline{E}(\overline{n},\overline{p})$ and is locally asymptotically stable. According to literature [19], the predator population density $\overline{p}$ can be expressed as a function of the prey population density $\overline{n}$:

$$\overline{p}=\sigma\overline{n}\left(1-\frac{\overline{n}}{k}\right),$$

and the prey population density $\overline{n}$ is the positive root of the following core constructed function $H(n)=0$:

$$H(n)=\frac{\alpha\sigma h_2}{k}n^4+\alpha\sigma\left(\frac{1-h_1}{k}-h_2\right)n^3+\left(\alpha\sigma(1-h_1)-h_2\right)n^2+(1-h_2)n-1=0.$$

Literature [19] specifically provides strict parameter conditions to ensure that the system has only one positive equilibrium point, provided that the following conditions are simultaneously satisfied:

1) $0<h_1<1$ and $0<h_2<\frac{(1-h_1)^2}{4}$,
2) $k\in(L_1,L_2)$,
3) $\alpha>\frac{h_2}{\sigma(1-h_1)}$.

Where the critical constants L_1 and L_2 are:

$$L_1=\frac{1-h_1-\sqrt{(1-h_1)^2-4h_2}}{2h_2},$$

$$L_2=\frac{1-h_1+\sqrt{(1-h_1)^2-4h_2}}{2h_2}.$$

The stability conditions are presented below. Under the premise of the existence of a unique equilibrium point, there exists a critical bifurcation value for the cooperative hunting intensity $\alpha_h\in[0,\alpha_m]$, where α_m is entirely determined by the carrying capacity k and the defense-related parameters h_1 and h_2. The formula is as follows:

$$\alpha_m=\frac{4(1-h_1-h_2k)}{\left(k\left(\frac{kh_2}{2}-1+h_1\right)\right)^2}.$$

Unlike α_m, the paper does not provide a simple, independent formula to directly calculate α_h; instead, α_h is defined as the root of an implicit equation:

$$V_1\left(\overline{n}(\alpha_h)\right)=0,$$

here, $V_1(n)$ is a highly complex polynomial concerning the prey density n and

the parameter α (corresponding to Equation 24 in literature [19]). When the parameter $\alpha \in (0, \alpha_h)$, the ODE model is locally asymptotically stable.

We can find the Jacobian matrix of the ODE model:

$$A = \begin{pmatrix} \overline{f}_n & \overline{f}_p \\ \overline{g}_n & \overline{g}_p \end{pmatrix},$$

here, $\overline{f}_n$ represents the value of the partial derivative of f with respect to n at $(\overline{n}, \overline{p})$, and similarly for the others. The parameter conditions for the stability of the equilibrium point have already been obtained. Under these conditions, we have $(H1)$: $\overline{f}_n + \overline{g}_p < 0$ and $(H2)$: $\overline{f}_n \overline{g}_p - \overline{f}_p \overline{g}_n > 0$, meaning that $(H1)$ and $(H2)$ are satisfied. Simple diffusion does not affect stability.

To analyze the stability of the system at the positive equilibrium $\overline{E}(\overline{n}, \overline{p})$, we introduce small perturbations

$$n(x,t) = \overline{n} + N(x,t) = \overline{n} + N,$$
$$n(x,t-\tau) = \overline{n} + N(x,t-\tau) = \overline{n} + N_\tau,$$
$$p(x,t) = \overline{p} + P(x,t) = \overline{p} + P,$$

the linearization of system (3) at the equilibrium point $(\overline{n}, \overline{p})$:

$$\begin{cases} N_t = d_1 N_{xx} + \overline{f}_n N + \overline{f}_p P, & x \in (0, L), t > 0, \\ P_t = d_2 P_{xx} - \chi \overline{\phi} P_{xx} + \overline{g}_n N_\tau + \overline{g}_p P, & x \in (0, L), t > 0, \\ N_x(x,t) = P_x(x,t) = 0, & x = 0, L, t > 0, \\ N(x,\theta) = N_0(x,\theta), \ P(x,\theta) = P_0(x,\theta), & x \in [0, L], \theta \in [-\tau, 0]. \end{cases} \tag{4}$$

where $\overline{\phi} = \phi(\overline{n}, \overline{p})$, here, $N_0(x,\theta)$ and $P_0(x,\theta)$ represent the small initial perturbation history functions around the equilibrium.

Here, the basis function used is $\cos\left(\frac{k\pi x}{L}\right)$. To analyze the stability of the linear equation, we expand the perturbation variables $N(x,t)$, $N(x,t-\tau)$ and $P(x,t)$ into the product form of a temporal exponential growth part and a spatial eigenfunction:

$$N(x,t) = c_1 e^{\lambda(t)} \cos\left(\frac{k\pi x}{L}\right),$$
$$N(x,t-\tau) = c_1 e^{\lambda(t-\tau)} \cos\left(\frac{k\pi x}{L}\right),$$
$$P(x,t) = c_2 e^{\lambda t} \cos\left(\frac{k\pi x}{L}\right),$$

here, c_1 and c_2 are the initial amplitude constants of the perturbation; λ is the eigenvalue representing the growth rate of the perturbation over time, which is usually a complex number; and $k = 0, 1, 2, \cdots$ is the wave number.

Let $\mu_k = \left(\frac{k\pi}{L}\right)^2$ denote the spatial eigenvalue. By substituting the above form of the solution into the various mathematical operators for simplification, it can

be written in matrix form:

$$\begin{pmatrix} \lambda + d_1\mu_k - \overline{f}_n & -\overline{f}_p \\ -\chi\overline{\phi}\mu_k - \overline{g}_n e^{-\lambda\tau} & \lambda + d_2\mu_k - \overline{g}_p \end{pmatrix} \begin{pmatrix} c_1 \\ c_2 \end{pmatrix} = \begin{pmatrix} 0 \\ 0 \end{pmatrix}. \tag{5}$$

The stability matrix of $(\overline{n}, \overline{p})$ is:

$$M_k = \begin{pmatrix} \lambda + d_1\mu_k - \overline{f}_n & -\overline{f}_p \\ -\chi\overline{\phi}\mu_k - \overline{g}_n e^{-\lambda\tau} & \lambda + d_2\mu_k - \overline{g}_p \end{pmatrix}. \tag{6}$$

Its characteristic equation corresponding to the eigenvalue λ is:

$$\begin{aligned} &\lambda^2 - \left[-\left(d_1 + d_2\right)\mu_k + \overline{f}_n + \overline{g}_p\right]\lambda + d_1 d_2 \mu_k^2 - \left(d_1\overline{g}_p + d_2\overline{f}_n + \overline{f}_p\chi\overline{\phi}\right)\mu_k \\ &+ \overline{f}_n\overline{g}_p - \overline{f}_p\overline{g}_n e^{-\lambda\tau} = 0. \end{aligned} \tag{7}$$

where

$$Tra_k = -\left(d_1 + d_2\right)\mu_k + \overline{f}_n + \overline{g}_p < 0,$$

and

$$Det_k(\tau) = d_1 d_2 \mu_k^2 - \left(d_1\overline{g}_p + d_2\overline{f}_n + \overline{f}_p\chi\overline{\phi}\right)\mu_k + \overline{f}_n\overline{g}_p - \overline{f}_p\overline{g}_n e^{-\lambda\tau}.$$

In the absence of time delay, letting $\tau = 0$, the characteristic equation reduces to $\lambda^2 - Tra_k\lambda + Det_k(0) = 0$. For all wave numbers $k \geq 0$, it is known that $Tra_k < 0$. For the system to remain stable, we must have $Det_k(0) > 0$, that is:

$$d_1 d_2 \mu_k^2 - \left(d_1\overline{g}_p + d_2\overline{f}_n + \overline{f}_p\chi\overline{\phi}\right)\mu_k + \overline{f}_n\overline{g}_p - \overline{f}_p\overline{g}_n > 0.$$

From this, we can directly solve for the critical taxis threshold χ_k that maintains spatial stability:

$$\chi_k = \frac{d_1 d_2 \mu_k^2 - \left(d_1\overline{g}_p + d_2\overline{f}_n\right)\mu_k + \overline{f}_n\overline{g}_p - \overline{f}_p\overline{g}_n}{\overline{f}_p\overline{\phi}\mu_k},$$

the stability analysis in literature [18] has proven that when $\chi < \min\chi_k$, $Det_k(0) > 0$ holds. The equilibrium point is locally asymptotically stable. The bifurcation analysis concerning $\tau > 0$ in the following section is conducted on the basis of incorporating the taxis term and the local asymptotic stability of the equilibrium solution.

3. Hopf Bifurcation Analysis with Delay

Based on the above characteristic Equation (7), we denote:

$$A_k = \left(d_1 + d_2\right)\mu_k - \overline{f}_n - \overline{g}_p > 0;$$

$$B_k(\chi) = d_1 d_2 \mu_k^2 - \left(d_1\overline{g}_p + d_2\overline{f}_n + \overline{f}_p\chi\overline{\phi}\right)\mu_k + \overline{f}_n\overline{g}_p;$$

$$C = -\overline{f}_p\overline{g}_n.$$

Therefore, the characteristic equation can be simplified as:

$$\lambda^2 + A_k\lambda + B_k(\chi) + Ce^{-\lambda\tau} = 0. \tag{8}$$

A necessary condition for the occurrence of a Hopf bifurcation is that the char-

acteristic equation has a pair of purely imaginary roots. Assuming $\lambda = i\beta_k$ (letting $\beta_k > 0$) is a root of the equation, substituting it into the characteristic Equation (8) yields:

$$\left(i\beta_k\right)^2 + A_k\left(i\beta_k\right) + B_k\left(\chi\right) + C\mathrm{e}^{-i\beta_k\tau} = 0, \tag{9}$$

by expanding using Euler's formula $\mathrm{e}^{-i\beta_k\tau} = \cos\left(\beta_k\tau\right) - i\sin\left(\beta_k\tau\right)$ and separating the real and imaginary parts of (9), we obtain:

$$\begin{cases} B_k\left(\chi\right) - \beta_k^2 + C\cos\left(\beta_k\tau\right) = 0, \\ A_k\beta_k - C\sin\left(\beta_k\tau\right) = 0. \end{cases} \tag{10}$$

Rearranging yields:

$$\begin{cases} C\cos\left(\beta_k\tau\right) = \beta_k^2 - B_k\left(\chi\right), \\ C\sin\left(\beta_k\tau\right) = A_k\beta_k. \end{cases} \tag{11}$$

Squaring the two equations in (11) respectively and adding them together, we use $\sin^2 + \cos^2 = 1$ to eliminate τ:

$$C^2 = \left(\beta_k^2 - B_k\left(\chi\right)\right)^2 + \left(A_k\beta_k\right)^2, \tag{12}$$

expanding and combining like terms yields a quartic polynomial with respect to β_k:

$$\beta_k^4 + \left(A_k^2 - 2B_k\left(\chi\right)\right)\beta_k^2 + B_k\left(\chi\right)^2 - C^2 = 0, \tag{13}$$

to reduce the degree, we let $\omega = \beta_k^2$, and (13) becomes a quadratic equation with respect to ω:

$$\omega^2 + P_k\omega + Q_k = 0, \tag{14}$$

where: $P_k = A_k^2 - 2B_k\left(\chi\right)$, $Q_k = B_k\left(\chi\right)^2 - C^2$.

For the system to undergo a Hopf bifurcation, there must exist at least one positive real root ω^*. If $Q_k < 0$, by Vieta's formulas, the equation must have one and only one positive real root $\omega_k^+ = \dfrac{-P_k + \sqrt{P_k^2 - 4Q_k}}{2}$. If $Q_k \geq 0$, $P_k < 0$, and the discriminant $\Delta = P_k^2 - 4Q_k \geq 0$, the equation has two positive real roots $\omega_k^\pm = \dfrac{-P_k \pm \sqrt{P_k^2 - 4Q_k}}{2}$.

These roots correspond to two distinct oscillation frequencies, $\beta_k^\pm = \sqrt{\omega_k^\pm}$, which in turn generate two separate sequences of critical time delays, denoted as $\tau_{k,j}^+$ and $\tau_{k,j}^-$. According to the transversality condition derived later in Equation (24), the sign of the real part derivative $\mathrm{d}\left(\mathrm{Re}\,\lambda\right)/\mathrm{d}\tau$ is strictly determined by the sign of $2\omega_k^\pm + P_k$. For the larger root ω_k^+, we have $2\omega_k^+ + P_k = \sqrt{\Delta} > 0$, indicating that the characteristic roots cross the imaginary axis from the left to the right half-plane, leading to a loss of stability. Conversely, for the smaller root ω_k^-, we have $2\omega_k^- + P_k = -\sqrt{\Delta} < 0$, meaning the roots cross from right to left, which may result in a stability switch. Therefore, the absolute first critical time delay τ^*—where the positive equilibrium initially loses its stability—is strictly defined by

the minimum of the delays associated with the destabilizing frequency branch β_k^+. Consequently, the Hopf bifurcation described in Theorem 3.1 applies specifically to the critical threshold determined by the ω_k^+ branch.

We have already determined the critical oscillation frequency $\beta_k = \sqrt{\omega_k} > 0$ that yields purely imaginary roots for the characteristic equation. Next, we need to find the corresponding critical time delay τ. Returning to the trigonometric system of Equation (11) obtained by separating the real and imaginary parts, we rearrange it to isolate the sine and cosine terms:

$$\begin{cases} \cos(\beta_k \tau) = \dfrac{\beta_k^2 - B_k(\chi)}{C}, \\ \sin(\beta_k \tau) = \dfrac{A_k \beta_k}{C}. \end{cases} \tag{15}$$

To uniquely determine the phase angle $\beta_k \tau \in [0, 2\pi)$, we need to strictly determine the signs of $\sin(\beta_k \tau)$ and $\cos(\beta_k \tau)$.

The coefficient of the linear term in the characteristic equation, $A_k = (d_1 + d_2)\mu_k - \overline{f}_n - \overline{g}_p$, is always greater than 0. Furthermore, since the oscillation frequency $\beta_k > 0$, the numerator $A_k \beta_k$ is always positive. Therefore, the sign of $\sin(\beta_k \tau)$ is completely determined by the sign of C: (i) If $C > 0$, then $\sin(\beta_k \tau) > 0$, which implies that the angle $\beta_k \tau$ must lie in either the first or the second quadrant, yielding

$$\theta_k = \arccos\left(\frac{\beta_k^2 - B_k(\chi)}{C}\right);$$

(ii) If $C < 0$, then $\sin(\beta_k \tau) < 0$, which indicates that the angle $\beta_k \tau$ must lie in the third or fourth quadrant, yielding

$$\theta_k = 2\pi - \arccos\left(\frac{\beta_k^2 - B_k(\chi)}{C}\right).$$

Due to the 2π-periodicity of trigonometric functions, there is more than one angle $\beta_k \tau$ satisfying the above equation, but rather infinitely many:

$$\beta_k \tau = \theta_k + 2j\pi, \quad j = 0, 1, 2, \cdots$$

Yielding

$$\tau_{k,j} = \frac{1}{\beta_k}(\theta_k + 2j\pi), \quad j = 0, 1, 2, \cdots$$

As the time delay τ gradually increases from 0, the system will lose stability at the first critical threshold it encounters. For any fixed wave number k, the minimum critical time delay obviously occurs when $j = 0$, namely $\tau_{k,0}$. Therefore, the absolute critical time delay τ^* for the system to undergo a Hopf bifurcation is the minimum value of $\tau_{k,0}$ over all possible spatial modes k:

$$\tau^* = \min_{k \in \mathbb{N}_0} \{\tau_{k,0}\}.$$

If τ^* is attained at $k = 0$, that is, $\tau^* = \tau_{0,0}$: the system undergoes a spatially

homogeneous Hopf bifurcation. At this time, the population density of the system will oscillate periodically in time, but remain uniform throughout the entire space; if τ^* is attained at $k>0$, that is, $\tau^*=\tau_{k,0}$: the system undergoes a spatially inhomogeneous Hopf bifurcation. In this case, the system not only oscillates in time but also exhibits pattern structures in space that fluctuate over time.

To rigorously prove that the system indeed undergoes a Hopf bifurcation as the time delay τ crosses the critical threshold $\tau_{k,j}$, we must verify the transversality condition. That is, we need to show that the derivative of the real part of the characteristic root with respect to τ is strictly greater than zero when crossing the imaginary axis, implying that the characteristic root crosses the imaginary axis at a non-zero rate.

Lemma 3.1. *Suppose that* $\omega_k=\beta_k^2$ *is a positive real root of the equation* $\omega^2+P_k\omega+Q_k=0$. *Let* $\lambda(\tau)=\alpha(\tau)+i\beta(\tau)$ *be the pair of complex roots of the system's characteristic equation near the critical point* $\tau=\tau_{k,j}$, *satisfying* $\alpha(\tau_{k,j})=0$ *and* $\beta(\tau_{k,j})=\beta_k$. *Then the following transversality condition holds:*

$$\left.\frac{\mathrm{d}(\mathrm{Re}\,\lambda)}{\mathrm{d}\tau}\right|_{\tau=\tau_{k,j}}>0.$$

Proof. We start from the characteristic equation of the system with respect to mode k:

$$\lambda^2+A_k\lambda+B_k(\chi)+C\mathrm{e}^{-\lambda\tau}=0, \tag{16}$$

treating λ as an implicit function of τ, differentiating both sides of Equation (16) with respect to τ yields:

$$2\lambda\frac{\mathrm{d}\lambda}{\mathrm{d}\tau}+A_k\frac{\mathrm{d}\lambda}{\mathrm{d}\tau}-C\mathrm{e}^{-\lambda\tau}\left(\frac{\mathrm{d}\lambda}{\mathrm{d}\tau}\tau+\lambda\right)=0, \tag{17}$$

factoring out $\frac{\mathrm{d}\lambda}{\mathrm{d}\tau}$ and rearranging yields:

$$\frac{\mathrm{d}\lambda}{\mathrm{d}\tau}\left(2\lambda+A_k-C\tau\mathrm{e}^{-\lambda\tau}\right)=C\lambda\mathrm{e}^{-\lambda\tau}. \tag{18}$$

To determine the sign of the real part more conveniently, we examine its reciprocal $\left(\frac{\mathrm{d}\lambda}{\mathrm{d}\tau}\right)^{-1}$:

$$\left(\frac{\mathrm{d}\lambda}{\mathrm{d}\tau}\right)^{-1}=\frac{2\lambda+A_k-C\tau\mathrm{e}^{-\lambda\tau}}{C\lambda\mathrm{e}^{-\lambda\tau}}=\frac{2\lambda+A_k}{C\lambda\mathrm{e}^{-\lambda\tau}}-\frac{\tau}{\lambda}. \tag{19}$$

From (16), we know that $C\mathrm{e}^{-\lambda\tau}=-\left(\lambda^2+A_k\lambda+B_k\right)$. Substituting this into the denominator of the above expression yields:

$$\left(\frac{\mathrm{d}\lambda}{\mathrm{d}\tau}\right)^{-1}=\frac{2\lambda+A_k}{-\lambda\left(\lambda^2+A_k\lambda+B_k\right)}-\frac{\tau}{\lambda}, \tag{20}$$

at the critical point $\tau=\tau_{k,j}$, the system has the purely imaginary root $\lambda=i\beta_k$. Substituting this into the above expression yields:

$$\left(\frac{\mathrm{d}\lambda}{\mathrm{d}\tau}\right)^{-1}\Bigg|_{\lambda=i\beta_k} = \frac{2i\beta_k + A_k}{-i\beta_k\left(-\beta_k^2 + A_k i\beta_k + B_k\right)} - \frac{\tau_{k,j}}{i\beta_k}, \tag{21}$$

simplifying it further, we expand the right-hand side of Equation (21) into its real and imaginary parts:

$$\frac{A_k + 2i\beta_k}{A_k\beta_k^2 + i\beta_k\left(\beta_k^2 - B_k\right)} + i\frac{\tau_{k,j}}{\beta_k}, \tag{22}$$

multiplying both the numerator and the denominator by the complex conjugate of the denominator, $A_k\beta_k^2 - i\beta_k\left(\beta_k^2 - B_k\right)$:

$$\begin{aligned}\mathrm{Re}\left[\left(\frac{\mathrm{d}\lambda}{\mathrm{d}\tau}\right)^{-1}\Bigg|_{\lambda=i\beta_k}\right] &= \frac{A_k\left(A_k\beta_k^2\right) + 2\beta_k\left[\beta_k\left(\beta_k^2 - B_k\right)\right]}{\left(A_k\beta_k^2\right)^2 + \beta_k^2\left(\beta_k^2 - B_k\right)^2} \\ &= \frac{A_k^2\beta_k^2 + 2\beta_k^2\left(\beta_k^2 - B_k\right)}{\beta_k^2\left[A_k^2\beta_k^2 + \left(\beta_k^2 - B_k\right)^2\right]} \\ &= \frac{2\beta_k^2 + A_k^2 - 2B_k}{A_k^2\beta_k^2 + \left(\beta_k^2 - B_k\right)^2}.\end{aligned} \tag{23}$$

Let $W = A_k^2\beta_k^2 + \left(\beta_k^2 - B_k\right)^2$. Since $\beta_k > 0$ and the parameters are not all zero, it is clear that $W > 0$. In the previous step, we let $\omega_k = \beta_k^2$ and defined $P_k = A_k^2 - 2B_k$. Substituting these into the numerator yields:

$$\mathrm{Re}\left[\left(\frac{\mathrm{d}\lambda}{\mathrm{d}\tau}\right)^{-1}\Bigg|_{\lambda=i\beta_k}\right] = \frac{2\omega_k + P_k}{W}. \tag{24}$$

substituting the expression of the positive root $\omega_k^+ = \frac{-P_k + \sqrt{P_k^2 - 4Q_k}}{2}$ into (24) and calculating yields:

$$2\omega_k^+ + P_k = 2\left(\frac{-P_k + \sqrt{P_k^2 - 4Q_k}}{2}\right) + P_k = \sqrt{P_k^2 - 4Q_k} > 0, \tag{25}$$

conclusion: Since $2\omega_k^+ + P_k > 0$, therefore

$$\mathrm{Re}\left[\frac{\mathrm{d}\lambda}{\mathrm{d}\tau}\Big|_{\lambda=i\beta_k,\tau=\tau_{k,j}}\right] > 0.$$

□

This rigorously proves that as the time delay τ increases and crosses the critical threshold $\tau_{k,j}$, the characteristic roots of the system cross the imaginary axis into the right half-plane at a positive rate, satisfying the transversality condition for a Hopf bifurcation.

Theorem 3.1. *If the system satisfies the preconditions for the local asymptotic stability of the positive equilibrium point, and the chemotaxis parameter is within the stable range, then for system (1.3), denoting the critical time delay as* $\tau^* = \min_{k\in\mathbb{N}_0}\left\{\tau_{k,0}\right\}$, *the following conclusions hold:*

1) When $\tau \in \left[0, \tau^*\right)$, the positive equilibrium point of the system is locally asymptotically stable.

2) When the time delay τ crosses the critical value τ^*, the characteristic roots of the system cross the imaginary axis into the right half-plane at a positive rate, and the positive equilibrium point loses stability.

a) When $\tau = \tau^*$ and $\tau^* = \tau_{0,0}$, that is, $k = 0$, the system undergoes a spatially homogeneous Hopf bifurcation at the positive equilibrium point. The population density oscillates periodically in time, but remains uniform throughout the entire space.

b) When $\tau = \tau^*$ and $\tau^* = \tau_{k,0}$, with $k > 0$, the system undergoes a spatially inhomogeneous Hopf bifurcation at the positive equilibrium point. The system not only oscillates in time, but also exhibits pattern structures in space that fluctuate over time.

4. Numerical Simulation

The numerical simulation employs the Method of Lines to decouple spatial and temporal variables, utilizing a second-order central finite difference scheme to discretize the partial differential equations into a high-dimensional system of delay differential equations, and relies on MATLAB's solver for time-stepping integration; additionally, the system sets the continuous history function as the positive equilibrium point subjected to a small perturbation using a uniform constant perturbation for spatially homogeneous simulations, and a localized Gaussian perturbation at the spatial midpoint for inhomogeneous simulations to break spatial symmetry thereby triggering and observing potential spatiotemporal patterns.

In this section, we will conduct numerical simulations using Matlab to visually verify the preceding theoretical analysis results regarding the local asymptotic stability of the system at the positive equilibrium point and the time delay-induced Hopf bifurcation. We select a set of benchmark parameters that satisfy the condition for the existence and uniqueness of the positive equilibrium point for the evolutionary analysis: $h_1 = 0.5$; $h_2 = 0.05$; $k = 3.0$; $\sigma = 1.0$; $\alpha = 0.01$; $d_1 = 0.1$; $d_2 = 0.1$; $L = 10.0$; $M = 0.8$; $\chi = 0.1$. With this set of parameters, the system is stable when $\tau = 0$, and the equilibrium point is found to be $(\overline{n}, \overline{p}) = (1.1089, 0.6990)$.

First, we calculated the critical time delay $\tau_{k,0}$ corresponding to the bifurcation of the system under spatial modes with different wave numbers k. As shown in Figure 1, the critical time delay changes as the wave number k varies, and the absolute critical time delay τ^* of the system depends on the minimum among these critical values.

To verify the first conclusion in Theorem 3.1, we select a time delay smaller than the critical threshold, namely $\tau = 0.20 < \tau^*$. As shown in Figure 2, after applying a small initial inhomogeneous perturbation at the spatial midpoint, the deviations in the population densities of the prey and predator gradually decay

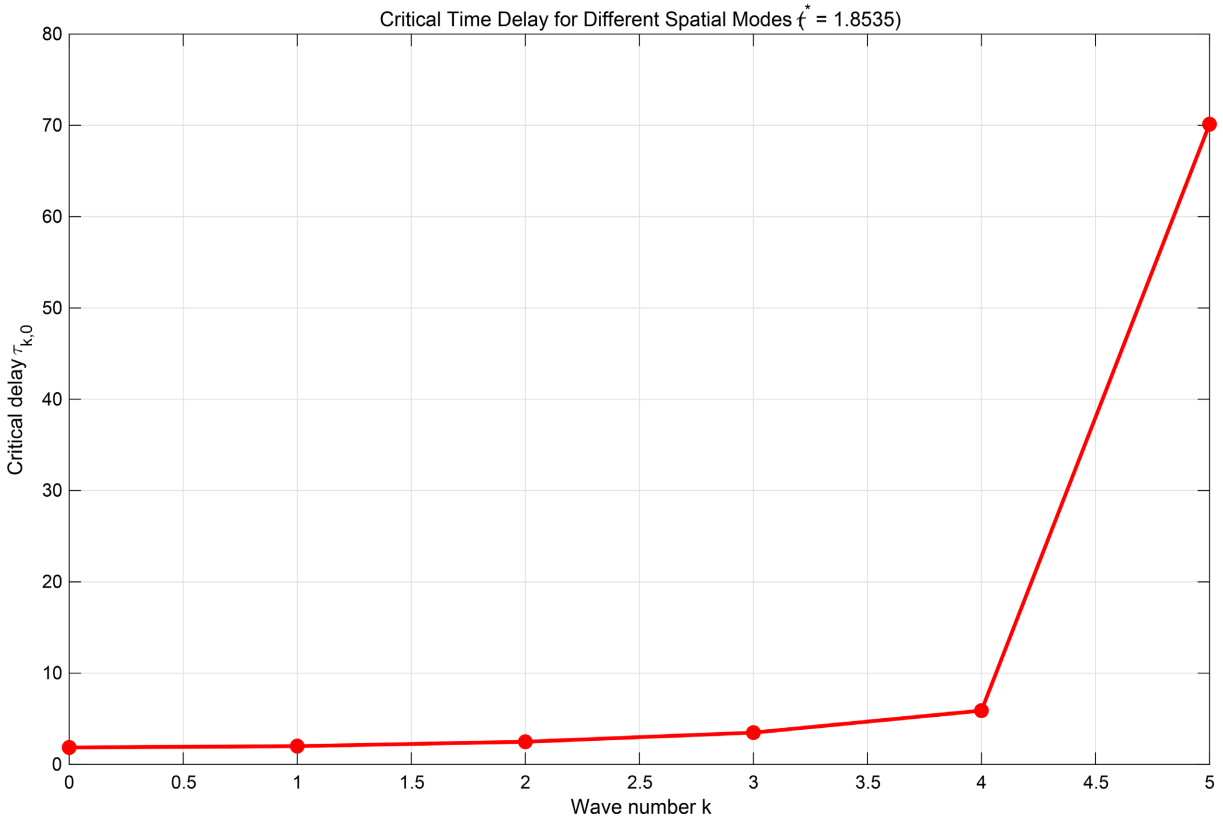

Figure 1. This figure illustrates the variation trend of the critical time delay $\tau_{k,0}$ corresponding to the occurrence of bifurcation in the system under spatial modes with different wave numbers k. The minimum critical value shown in the figure is $\tau^* = 1.8535$.

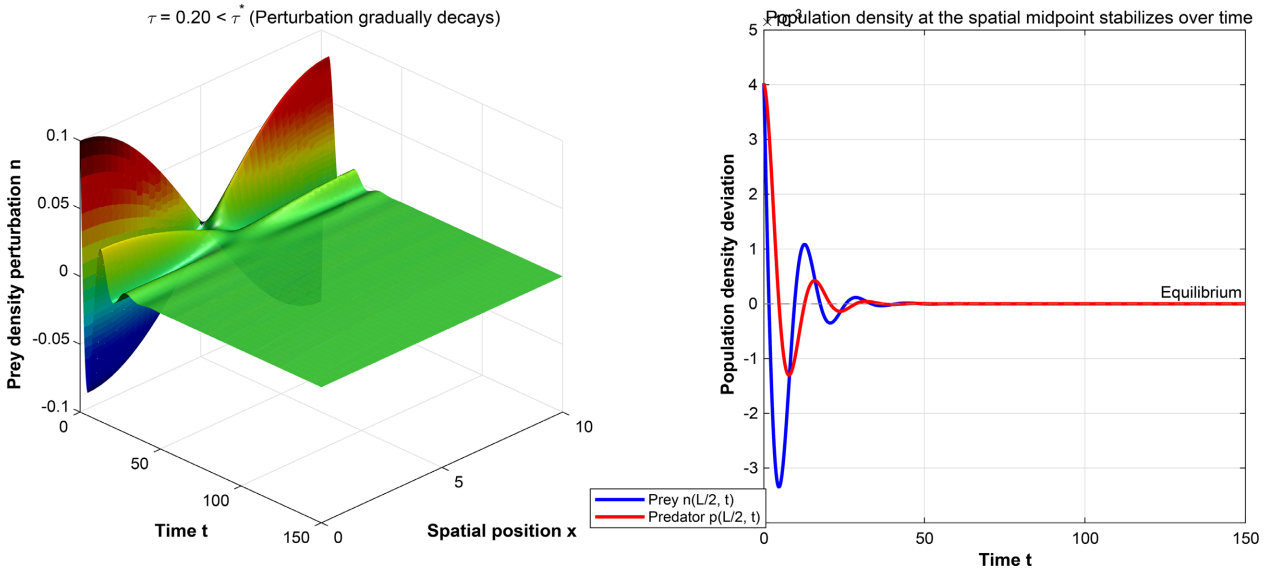

Figure 2. This shows that when the time delay is small, the system gradually decays after a small perturbation and converges to the equilibrium point, maintaining a stable spatially homogeneous coexistence state.

over time, eventually converging and stabilizing at zero. This indicates that under a small time delay, the chemotaxis system can still maintain a stable spatially homogeneous coexistence state.

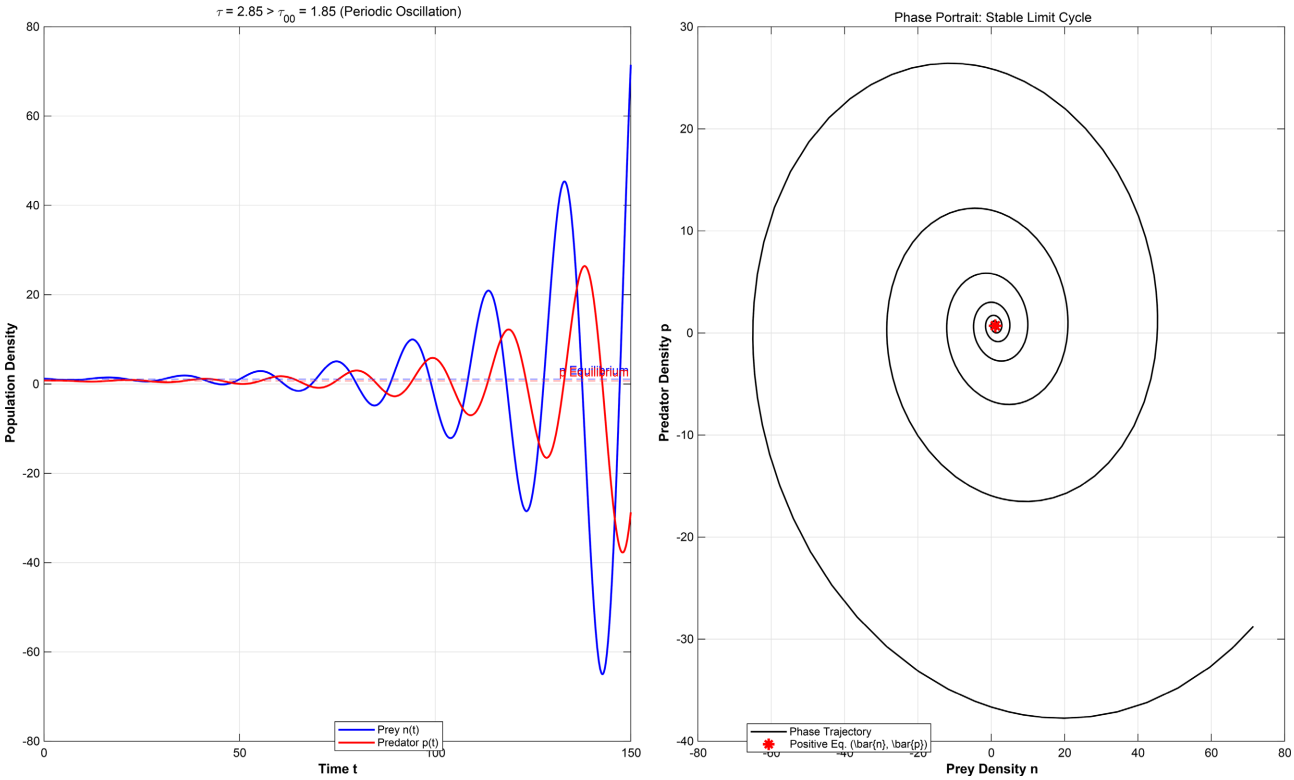

Figure 3. This shows that when the wave number $k = 0$ and the time delay crosses the critical value, the system undergoes a spatially homogeneous Hopf bifurcation, where the population density exhibits sustained periodic oscillations and forms a stable limit cycle.

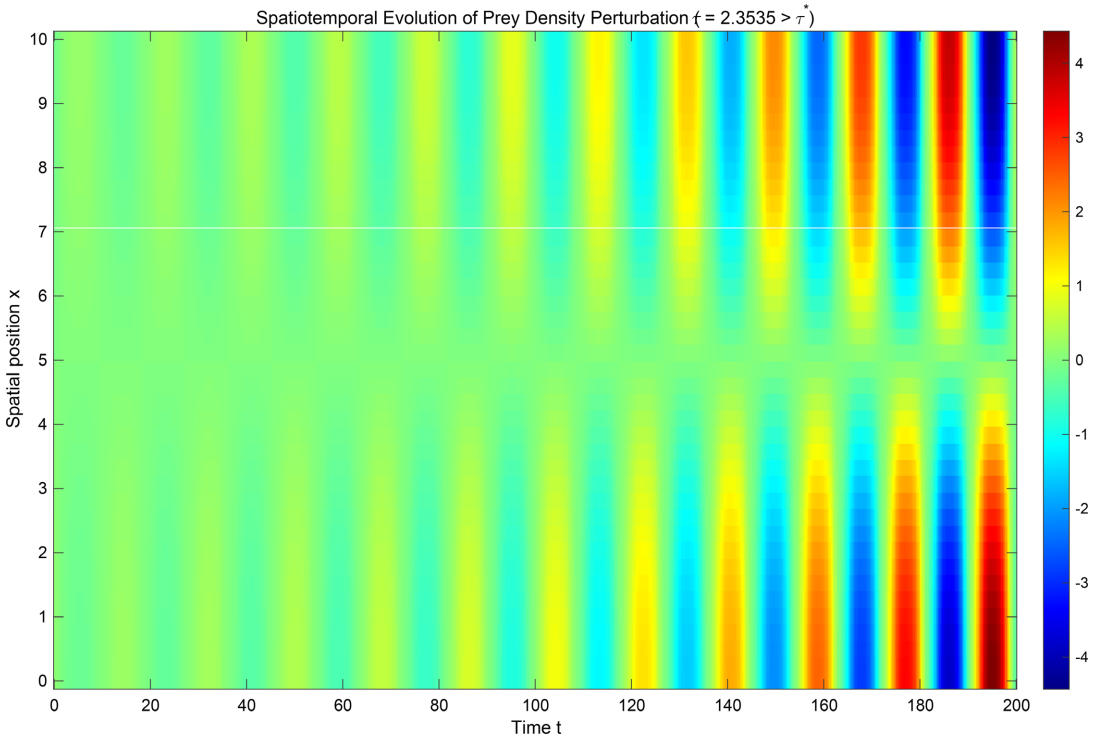

Figure 4. This shows that when the time delay is large ($\tau = 2.3535 > \tau^*$), the steady state of the system is completely destroyed, spontaneously evolving into spatially inhomogeneous, periodic wave-like patterns.

When we select $\tau = 2.85 > \tau_{0,0} = 1.85$ in the mode without spatial diffusion (*i.e.*, $k = 0$), the characteristic roots of the system cross the imaginary axis, and the positive equilibrium point loses stability. As shown in the time series plot on the left side of Figure 3, the population densities of the prey and predator exhibit sustained, non-decaying periodic oscillations. The phase plane portrait on the right side of Figure 3 further clearly shows that the phase trajectories of the system are eventually attracted to and form a stable limit cycle around the positive equilibrium point. This verifies the conclusion of Theorem 3.1(a).

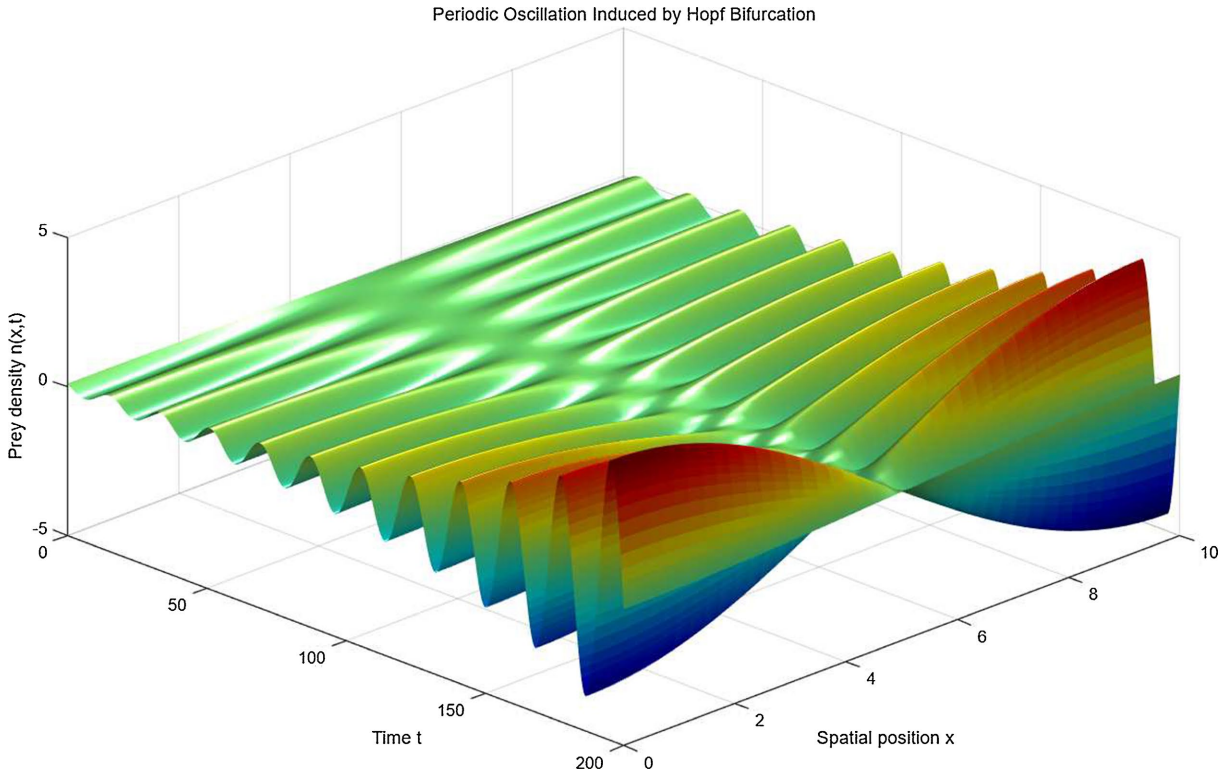

Figure 5. This shows the three-dimensional surface.

To investigate the effect of a larger time delay on spatial heterogeneity, we further select $\tau = 2.3535 > \tau^*$. As illustrated by the two-dimensional spatio-temporal evolution top view in Figure 4 and the three-dimensional evolution surface in Figure 5, the larger time delay completely destroys the steady-state coexistence of the populations. The system is not only excited into periodic oscillations in the temporal dimension, but also spontaneously forms distinct wave-like inhomogeneous distributions in the spatial dimension. This spatially inhomogeneous periodic solution, induced by the Hopf bifurcation, fully reveals the complex spatio-temporal evolutionary dynamics of the ecosystem under the combined effects of time delay and chemotaxis.

Conflicts of Interest

The author declares no conflicts of interest regarding the publication of this paper.

References

[1] Skellam, J.G. (1951) Random Dispersal in Theoretical Populations. *Biometrika*, **38**, 196-218. https://doi.org/10.1093/biomet/38.1-2.196

[2] Kareiva, P. and Odell, G. (1987) Swarms of Predators Exhibit "Preytaxis" If Individual Predators Use Area-Restricted Search. *The American Naturalist*, **130**, 233-270. https://doi.org/10.1086/284707

[3] Zhang, L. and Fu, S. (2019) Global Bifurcation for a Holling-Tanner Predator-Prey Model with Prey-Taxis. *Nonlinear Analysis*: *Real World Applications*, **47**, 460-472. https://doi.org/10.1016/j.nonrwa.2018.12.002

[4] Banda, H., Chapwanya, M. and Dumani, P. (2022) Pattern Formation in the Holling-tanner Predator-Prey Model with Predator-Taxis. A Nonstandard Finite Difference Approach. *Mathematics and Computers in Simulation*, **196**, 336-353. https://doi.org/10.1016/j.matcom.2022.01.028

[5] Wang, K., Wang, Q. and Yu, F. (2015) Stationary and Time Periodic Patterns of Two-Predator and One-Prey Systems with Prey-Taxis.

[6] Mishra, P. and Wrzosek, D. (2022) Repulsive Chemotaxis and Predator Evasion in Predator-Prey Models with Diffusion and Prey-Taxis. *Mathematical Models and Methods in Applied Sciences*, **32**, 1-42. https://doi.org/10.1142/s0218202522500014

[7] Yang, K. (1993) Delay Differential Equations: With Applications in Population Dynamics. Vol. 191, Academic Press.

[8] Anokye, M., Guerrini, L., Ferrara, M., Sackitey, A.L. and Konadu, A.A. (2026) Stability and Bifurcation in a Delayed Predator-Prey Model with Environmental Stress and Dynamic Carrying Capacity. *Differential Equations and Dynamical Systems*. https://doi.org/10.1007/s12591-026-00765-1

[9] Liu, Y. and Wei, X. (2025) Hopf Bifurcation Analysis in a Reaction-Diffusion-Advection Model with Strong Allee Effect and Delay. *AIMS Mathematics*, **11**, 11559-11579.

[10] Chen, M. and Srivastava, H.M. (2023) Stability of Bifurcating Solution of a Predator-Prey Model. *Chaos*, *Solitons & Fractals*, **168**, Article ID: 113153. https://doi.org/10.1016/j.chaos.2023.113153

[11] Yang, R. and Zhang, C. (2016) Dynamics in a Diffusive Predator-Prey System with a Constant Prey Refuge and Delay. *Nonlinear Analysis*: *Real World Applications*, **31**, 1-22. https://doi.org/10.1016/j.nonrwa.2016.01.005

[12] Pati, N.C. and Ghosh, B. (2022) Delayed Carrying Capacity Induced Subcritical and Supercritical Hopf Bifurcations in a Predator-Prey System. *Mathematics and Computers in Simulation*, **195**, 171-196. https://doi.org/10.1016/j.matcom.2022.01.008

[13] Wang, J., Wu, S. and Shi, J. (2021) Pattern Formation in Diffusive Predator-Prey Systems with Predator-Taxis and Prey-Taxis. *Discrete and Continuous Dynamical Systems-B*, **26**, 1273-1289. https://doi.org/10.3934/dcdsb.2020162

[14] Yoon, C., Wu, S. and Shi, J. (2022) Global Dynamics of a Lotka-Volterra Type Prey-predator Model with Diffusion and Predator-Taxis. *Applicable Analysis*, **101**, 5557-5570. https://doi.org/10.1080/00036811.2021.1898598

[15] He, X. and Zheng, S. (2015) Global Boundedness of Solutions in a Reaction-Diffusion System of Predator-Prey Model with Prey-Taxis. *Applied Mathematics Letters*, **49**, 73-77. https://doi.org/10.1016/j.aml.2015.04.017

[16] Zuo, W. and Wei, J. (2011) Stability and Hopf Bifurcation in a Diffusive Predator-Prey System with Delay Effect. *Nonlinear Analysis*: *Real World Applications*, **12**, 1998-2011. https://doi.org/10.1016/j.nonrwa.2010.12.016

[17] Teixeira Alves, M. and Hilker, F.M. (2017) Hunting Cooperation and Allee Effects in Predators. *Journal of Theoretical Biology*, **419**, 13-22. https://doi.org/10.1016/j.jtbi.2017.02.002

[18] Wang, Q., Song, Y. and Shao, L. (2017) Nonconstant Positive Steady States and Pattern Formation of 1D Prey-Taxis Systems. *Journal of Nonlinear Science*, **27**, 71-97. https://doi.org/10.1007/s00332-016-9326-5

[19] Benamara, I. and El Abdllaoui, A. (2023) Bifurcation in a Delayed Predator-Prey Model with Holling Type IV Functional Response Incorporating Hunting Cooperation and Fear Effect. *International Journal of Dynamics and Control*, **11**, 2733-2750. https://doi.org/10.1007/s40435-023-01123-7